NASA TECHNICAL NOTE

NASA TN D-7803

OPTIMIZATION OF SELF-ACTING HERRINGBONE-GROOVED JOURNAL BEARINGS FOR MAXIMUM STABILITY

by David P. Fleming and Bernard J. Hamrock

Lewis Research Center

Cleveland, Ohio 44135

NATIONAL AERONAUTICS AND SPACE ADMINISTRATION • WASHINGTON, D. C. • OCTOBER 1974

1. Report No. NASA TN D-7803	2. Government Accession No.	3. Recipient's Catalog No.
4. Title and Subtitle OPTIMIZATION OF SELF-ACTING HERRINGBONE-GROOVED JOURNAL BEARINGS FOR MAXIMUM STABILITY		5. Report Date OCTOBER 1974
		6. Performing Organization Code
7. Author(s) David P. Fleming and Bernard J. Hamrock		8. Performing Organization Report No. E-7793
9. Performing Organization Name and Address Lewis Research Center National Aeronautics and Space Administration Cleveland, Ohio 44135		10. Work Unit No. 501-24
		11. Contract or Grant No.
12. Sponsoring Agency Name and Address National Aeronautics and Space Administration Washington, D.C. 20546		13. Type of Report and Period Covered Technical Note
		14. Sponsoring Agency Code

15. Supplementary Notes

16. Abstract

Groove parameters were determined to maximize the stability of herringbone-grooved journal bearings. Parameters optimized were groove depth, width, length, and angle. Optimization was performed by using a small-eccentricity, infinite-groove analysis in conjunction with (1) a previously developed Newton-Raphson procedure for bearings with the smooth member rotating or with the grooved member rotating at low compressibility numbers and (2) a newly developed vector technique for bearings with the grooved member rotating at high compressibility numbers. The design curves in this report enable one to choose the optimum bearing for a wide range of operating conditions. These include (1) compressibility numbers from 0 (incompressible) to 80, (2) length-to-diameter ratios from 1/4 to 2, and (3) rotation of the smooth or grooved member. Compared with bearings optimized to maximize load capacity, bearings optimized for stability (1) allow a thousandfold increase in bearing-supported mass in some cases before onset of instability (the most pronounced increases are for bearings with small length-to-diameter ratios operating at high compressibility numbers) and (2) lose no more than 77 percent of their load capacity in any case studied. Stability is much greater when the grooved member rotates.

17. Key Words (Suggested by Author(s)) Gas lubrication Journal bearing stability Optimization procedures Herringbone-grooved bearings	18. Distribution Statement Unclassified - unlimited Category 15		
19. Security Classif. (of this report) Unclassified	20. Security Classif. (of this page) Unclassified	21. No. of Pages 22	22. Price* $3.00

OPTIMIZATION OF SELF-ACTING HERRINGBONE-GROOVED JOURNAL

BEARINGS FOR MAXIMUM STABILITY

by David P. Fleming and Bernard J. Hamrock

Lewis Research Center

SUMMARY

Groove parameters were determined to maximize the stability of herringbone-grooved journal bearings. Parameters optimized were groove depth, width, length, and angle. Optimization was performed by using a small-eccentricity, infinite-groove analysis in conjunction with (1) a previously developed Newton-Raphson procedure for bearings with the smooth member rotating or with the grooved member rotating at low compressibility numbers and (2) a newly developed vector technique for bearings with the grooved member rotating at high compressibility numbers.

The design curves in this report enable one to choose the optimum bearing for a wide range of operating conditions. These include (1) compressibility numbers from 0 (incompressible) to 80, (2) length-to-diameter ratios from 1/4 to 2, and (3) rotation of the smooth or grooved member.

Compared with bearings optimized to maximize load capacity, bearings optimized for stability (1) allow a thousandfold increase in bearing-supported mass in some cases before onset of instability (the most pronounced increases are for bearings with small length-to-diameter ratios operating at high compressibility numbers) and (2) lose no more than 77 percent of their load capacity in any case studied. Stability is much greater when the grooved member rotates.

INTRODUCTION

More than any other factors, self-excited whirl instability and low load capacity limit the usefulness of gas-lubricated self-acting journal bearings. The whirl problem is the tendency of the journal center to orbit the bearing center at an angular speed less than or equal to half that of the journal about its own center. In many cases the whirl amplitude is large enough to cause destructive contact of the bearing surfaces.

The low load capacity of self-acting gas-lubricated journal bearings is also a serious concern in many applications, largely because of the low viscosity of gases. Also, unlike a liquid lubricant, a gaseous lubricant changes its density as it passes through the bearing. This so-called compressibility effect results in a "terminal" load condition. That is, the load capacity does not increase indefinitely with speed, but quickly approaches a fixed value.

In quest of a bearing which would overcome the two problems of self-excited whirl instability and low load capacity, Vohr and Chow (ref. 1) theoretically investigated a herringbone-grooved journal bearing. They obtained a solution for bearing load capacity valid for small displacements of the journal center from the bearing center. An additional assumption was that the number of grooves was large enough that local pressure variations across a groove-ridge pair could be ignored. One of the conclusions obtained from the Vohr and Chow analysis is that, in contrast to the behavior of a plain bearing, the load capacity of a herringbone-grooved journal bearing increases without limit with increase in speed. Furthermore, the herringbone-grooved journal bearing may not suffer from the self-excited whirl instability that is normally associated with unloaded plain bearings. Malanoski (ref. 2) and Cunningham, Fleming, and Anderson (refs. 3 and 4) experimentally verified these conclusions of Vohr and Chow.

Therefore, the self-acting herringbone journal bearing has at least two highly desirable characteristics, namely, high load capacity and the capability of operating in a whirl free condition. A remaining problem is that of obtaining optimum herringbone journal bearing configurations for a wide range of bearing operating conditions. Hamrock and Fleming (ref. 5) determined groove parameters to maximize the radial load component of the herringbone bearing. The objective of the present work is to determine groove parameters which will maximize the stability of the bearing, or the resistance to self-excited whirl. This will be done by utilizing the analysis of Vohr and Chow (ref. 1). Results are to be applicable for operating conditions ranging from incompressible to highly compressible lubrication ($\Lambda = 80$) and for bearing length-to-diameter ratios of 1/4 to 2.

SYMBOLS

A, B	numerical factors
b_g	width of groove
b_r	width of ridge
C	coefficient in differential equation
D	diameter of journal

$\overline{E}$ change in groove parameter vector

e eccentricity of journal

F_r dimensionless radial load component, $f_r/\epsilon p_a LD$ for compressible lubricant, $2f_r h_r^2 / 3\mu\epsilon LD^3\omega$ for incompressible lubricant

f_r, f_t radial and tangential load components of bearing

G complex function of Z

H film thickness ratio, h_g/h_r

h_g film thickness in groove region when journal is concentric

h_r film thickness in ridge region when journal is concentric

L length of journal

L_1 total axial length of groove

M dimensionless stability parameter, $mp_a(h_r/R)^5/2L\mu^2$ for compressible lubricant, $3m\omega(h_r/R)^3/L\mu = M_{comp}\Lambda$ for imcompressible lubricant

m mass supported by bearing

N number of grooves

p pressure

p_a ambient pressure

R radius of journal

Re real part of expression

t time

Z axial coordinate

α groove width ratio, $b_g/(b_g + b_r)$

β groove angle

γ groove length ratio, L_1/L

ϵ eccentricity ratio, e/h_r

$\theta, \theta*$ angular coordinates

Λ bearing compressibility number, $6\mu\omega R^2/p_a h_r^2$

μ dynamic viscosity of lubricant

ξ groove rotation indicator, +1 for smooth member rotating, -1 for grooved member rotating

ω rotational speed

ω_p whirl speed

∇ gradient operator

BEARING DESCRIPTION

Figure 1 shows the bearing to be studied. Note that the bearing has angled, shallow grooves in the journal surface. The grooves can be partial as shown or extend the complete length of the bearing. Also, the grooves can be placed in the rotating or non-rotating surface. The purpose of these grooves is to pump fluid toward the center of the bearing and thereby increase the lubricant pressure in the bearing. This self-pressurization can increase the load capacity over that of a smooth bearing; it is also responsible for the good stability of the herringbone bearing. The herringbone bearing is unidirectional; that is, it pumps inwardly for only one direction of rotation.

From figure 1 the film thickness in the groove region is h_g and in the ridge region is h_r. Also, the groove width is defined as b_g, and the ridge width is defined as b_r. The analysis to be described indicates that the groove parameters to be optimized are

    (1) Film thickness ratio H, which is equal to the film thickness in the groove region divided by the film thickness in the ridge region when the bearing is concentric ($H = h_g/h_r$)

    (2) Groove width ratio α, which is equal to the width of the groove region divided by the width of the groove-ridge pair ($\alpha = b_g/(b_g + b_r)$)

    (3) Groove angle β

    (4) Groove length ratio γ, which is equal to the length covered by grooves divided by the overall length of the bearing ($\gamma = L_1/L$)

ANALYSIS

Equations for Herringbone-Grooved Bearing

Vohr and Chow (ref. 1), by assuming a large number of grooves, obtained relations for a "smoothed" pressure in the bearing film. That is, they dealt with an overall pressure rather than treating separately the pressure in the grooves and that over the ridges. To conveniently obtain solutions for steady whirling, which are needed for the stability analysis, they introduced a rotating coordinate system by

$$\theta^* = \theta - \omega_p t \qquad (1)$$

where ω_p is the frequency of steady circular whirling. They next assumed that the smoothed pressure $p(\theta^*, Z)$ could be represented by

$$p(\theta^*, Z) = p_0(Z) + \epsilon p_1(\theta^*, Z) \tag{2}$$

This is the well known small-eccentricity perturbation solution.

When equation (2) is substituted into the expressions for smoothed pressure, and terms are collected according to the powers of ϵ, separate expressions result for p_0 and p_1:

$$\frac{dp_0}{dZ} = C_p \frac{p_a}{L} \tag{3}$$

$$C_1 \frac{L^2}{p_a} \frac{\partial^2 p_1}{\partial Z^2} + C_2 \frac{L}{p_a} \frac{\partial p_1}{\partial Z} + C_3 \frac{L}{p_a} \frac{\partial^2 p_1}{\partial Z \partial \theta^*} + \frac{C_4}{p_a} \frac{\partial p_1}{\partial \theta^*} + \frac{C_5}{p_a} \frac{\partial^2 p_1}{\partial \theta^{*2}} + C_6 \sin \theta^* + C_7 \cos \theta^* = 0 \tag{4}$$

The coefficients C_p and C_1 to C_7 are given in the appendix. They differ slightly from the coefficients appearing in reference 1 because only one bearing member (grooved or smooth) is in motion. Equation (3) may be integrated directly. Equation (4) may be reduced to an ordinary differential equation by using the product solution

$$p_1 = \mathcal{R}e(G(Z)e^{i\theta^*}) \tag{5}$$

Since $\cos \theta = \mathcal{R}e(e^{i\theta})$ and $\sin \theta = \mathcal{R}e(-ie^{i\theta})$, the substitution of equation (5) in equation (4) results in

$$C_1 \frac{L^2}{p_a} \frac{d^2 G}{dZ^2} + (C_2 + iC_3) \frac{L}{p_a} \frac{dG}{dZ} + (iC_4 - C_5) \frac{G}{p_a} - iC_6 + C_7 = 0 \tag{6}$$

Equation (6) may be integrated numerically by a forward difference scheme such as Runge-Kutta. Further details on the solution procedure are given in references 6 and 7.

These equations were derived for gas lubrication. However, they may also be used for incompressible lubricants by setting C_2, C_4, and C_7 equal to zero.

In figure 1 the number of grooves is six. However, the Vohr and Chow analysis (ref. 1) assumes essentially an infinite number of grooves. Reference 6 develops the following criterion for a minimum number of grooves such that the infinite-groove analysis yields valid results:

$$\frac{\Lambda}{N} < \frac{[(1 - \alpha)H^3 + \alpha][H^3 + \alpha(1 - \alpha)(H^3 - 1)^2 \sin^2\beta]}{2\pi[H^3 + \alpha(1 - \alpha)(H^3 - 1)^2]\alpha(1 - \alpha)(H - 1)\sin^2\beta} \tag{7}$$

where

Λ bearing compressibility number, $6\mu\omega R^2 / p_a h_r^2$

N number of grooves

The numerical value of the right side of inequality (7) is typically between 5.5 and 8.0. Therefore, the minimum number of grooves to be used can be represented conservatively by

$$N \geq \frac{\Lambda}{5} \tag{8}$$

Stability Determination

Once equations (2) to (6) are solved for the pressure p, the bearing load may be calculated for any whirl frequency ω_p. Stability is then determined by using the spectral analysis method of Pan (ref. 8). In this method, the assumed whirl frequency is varied until the bearing tangential force f_t equals zero. (It is this tangential force which causes an unloaded bearing to begin whirling - see fig. 2.) The bearing neutral stability condition is then found by equating the centrifugal force, due to the whirling bearing mass (i.e., the mass supported by the bearing), to the bearing radial force:

$$me\omega_p^2 = f_r \tag{9}$$

It is convenient to define dimensionless bearing masses according to

$$M = \frac{mp_a}{2L\mu^2}\left(\frac{h_r}{R}\right)^5 \tag{10a}$$

for a compressibly lubricated bearing and

$$M = \frac{3m\omega}{L\mu}\left(\frac{h_r}{R}\right)^3 \tag{10b}$$

for an incompressibly lubricated bearing.

6

OPTIMIZING PROCEDURE

The problem is to maximize the bearing stability M by optimizing the groove parameters H, α, β, and γ. As mentioned in the last section, the small-eccentricity analysis of Vohr and Chow (ref. 1) is used. Stability is then determined for a particular configuration by the spectral analysis method of Pan (ref. 8). Basically, two different optimizing procedures are used, depending on the characteristics of the particular bearing being optimized.

Zero Derivative Method

For the bearing having the smooth member rotating and for the bearing with the grooved member rotating with low compressibility numbers, the method of reference 5 was used. In this method, one determines groove parameters such that

$$\frac{\partial M}{\partial H} = \frac{\partial M}{\partial \alpha} = \frac{\partial M}{\partial \beta} = \frac{\partial M}{\partial \gamma} = 0 \tag{11}$$

by using the Newton-Raphson procedure of solving simultaneous equations. This procedure is described in reference 9; in addition to its use in reference 5, it was used in optimizing a Rayleigh step thrust bearing (ref. 10). Briefly, the method consists of letting

$$\left.\begin{aligned} H &= \overline{H} + \Delta H \\ \alpha &= \overline{\alpha} + \Delta \alpha \\ \beta &= \overline{\beta} + \Delta \beta \\ \gamma &= \overline{\gamma} + \Delta \gamma \end{aligned}\right\} \tag{12}$$

where $\overline{H}$, $\overline{\alpha}$, $\overline{\beta}$, and $\overline{\gamma}$ are initial estimates of the optima to satisfy equation (11), and ΔH, $\Delta \alpha$, $\Delta \beta$, and $\Delta \gamma$ are correction terms. Substituting equations (12) into equation (11) and expanding these equations by Taylor's theorem for a function of four variables while neglecting second-order and higher order terms give the following:

$$\frac{\partial M}{\partial H} + \Delta H \frac{\partial^2 M}{\partial H^2} + \Delta\alpha \frac{\partial^2 M}{\partial H\, \partial\alpha} + \Delta\beta \frac{\partial^2 M}{\partial H\, \partial\beta} + \Delta\gamma \frac{\partial^2 M}{\partial H\, \partial\gamma} = 0$$

$$\frac{\partial M}{\partial\alpha} + \Delta H \frac{\partial^2 M}{\partial\alpha\, \partial H} + \Delta\alpha \frac{\partial^2 M}{\partial\alpha^2} + \Delta\beta \frac{\partial^2 M}{\partial\alpha\, \partial\beta} + \Delta\gamma \frac{\partial^2 M}{\partial\alpha\, \partial\gamma} = 0$$

$$\frac{\partial M}{\partial\beta} + \Delta H \frac{\partial^2 H}{\partial\beta\, \partial H} + \Delta\alpha \frac{\partial^2 M}{\partial\beta\, \partial\alpha} + \Delta\beta \frac{\partial^2 M}{\partial\beta^2} + \Delta\gamma \frac{\partial^2 M}{\partial\beta\, \partial\gamma} = 0$$

$$\frac{\partial M}{\partial\gamma} + \Delta H \frac{\partial^2 M}{\partial\gamma\, \partial H} + \Delta\alpha \frac{\partial^2 M}{\partial\gamma\, \partial\alpha} + \Delta\beta \frac{\partial^2 M}{\partial\gamma\, \partial\beta} + \Delta\gamma \frac{\partial^2 M}{\partial\gamma^2} = 0$$

$$\left.\rule{0pt}{120pt}\right\} \qquad (13)$$

The partial derivatives in equation (13) can be expressed in terms of a finite-difference formulation. The correction terms ΔH, $\Delta\alpha$, $\Delta\beta$, and $\Delta\gamma$ are then found by using determinants. Additional corrections can be obtained by repeated application of equations (12) and (13), where the initial values $\overline{H}$, $\overline{\alpha}$, $\overline{\beta}$, and $\overline{\gamma}$ are then the values of H, α, β, and γ given by equation (12) of the preceding evaluation.

When the smooth member of the bearing rotates, or the grooved member rotates with low compressibility number Λ, the stability decreases monotonically with increasing Λ, as shown in figure 3(a). With the grooved member rotating, stability is not always monotonic at higher Λ, as shown in figure 3(b). (These characteristics are also shown in ref. 2.) Thus, if one imposes the requirement that a bearing must operate at all Λ values less than the value in question (as the bearing must certainly be started and stopped occasionally), it follows that a proper optimization must maximize the minimum value of stability from $\Lambda = 0$ to the Λ of interest. This being the case, the Newton-Raphson method as used previously will not produce the desired results.

Two cases present themselves. In the first, for moderate compressibility numbers (e.g., $\Lambda = 10$ for $L/D = 2$) the optimum stability curve is of the form shown as the long-and-short-dash curve in figure 3(b). If one needs to operate at a maximum Λ of 10, the minimum stability at $\Lambda = 5.6$ is the governing factor. In this case, the Newton-Raphson optimization can be applied at the Λ value where the minimum stability occurs. Since a change in groove parameters may change the Λ value where minimum stability occurs, this Λ value is recomputed at each iteration by using a Newton-Raphson root finder.

For operation at high compressibility numbers a completely different technique is required, as will be illustrated. Refer to the solid curve of figure 3(b). For these groove parameters, stability decreases with increasing Λ at low values of Λ. A relative minimum is reached at $\Lambda = 6$; M then increases and becomes unbounded near $\Lambda = 26$. Another relative minimum occurs at $\Lambda = 38$, and M is again unbounded near $\Lambda = 54$. Stability then decreases rapidly with increasing Λ.

In attempting to optimize the bearing, one finds that, if the groove parameters are adjusted to increase the relative minimum at $\Lambda = 6$, the stability at $\Lambda = 80$ decreases. Thus, one must look simultaneously at the stability at the Λ of interest and at any relative minima within the range.

The methods of vector analysis are used here. The greatest rate of change of a function occurs along the gradient of that function. Refer again to the solid curve of figure 3(b) and denote by Λ_m and M_m the compressibility number and stability at the relative minimum ($\Lambda = 6$ in fig. 3(b)). Denote by Λ_1 and M_1 the compressibility number and stability at the compressibility number of interest ($\Lambda = 80$ in this example). In light of the foregoing discussion, it is evident that maximum stability over the range 0 to Λ_1 will be attained when $M_m = M_1$. The technique is then to calculate the gradient of M at $\Lambda = \Lambda_m$ and $\Lambda = \Lambda_1$. A change is then made in the vector of independent variables (H, α, β, and γ) by taking a linear combination of the two gradients just calculated so that the new M_m and M_1 will be equal and increased over the original values. This procedure is applied repeatedly, until further application no longer increases M_m and M_1.

The specific expressions to carry out this technique will now be presented. Denote by M_p the new value of M at Λ_1 and Λ_m, and denote by $\overline{E}$ the change in the vector of independent variables. Then

$$M_p = M_1 + \overline{E} \cdot \nabla M_1 = M_m + \overline{E} \cdot \nabla M_m \tag{14}$$

where the gradient ∇M is given by

$$\nabla M = \left(\frac{\partial M}{\partial H}, \ \frac{\partial M}{\partial \alpha}, \ \frac{\partial M}{\partial \beta}, \ \frac{\partial M}{\partial \gamma} \right) \tag{15}$$

But $\overline{E}$ is to be a linear combination of the two gradients:

$$\overline{E} = A \ \nabla M_1 + B \ \nabla M_m \tag{16}$$

where A and B are scalars. Equations (14) and (16) are combined and solved for B:

$$B = \frac{M_1 - M_m - A \nabla M_1 \cdot (\nabla M_1 - \nabla M_m)}{\nabla M_m \cdot (\nabla M_1 - \nabla M_m)} \tag{17}$$

In the computer program used to perform the calculations, A is first chosen equal to 1 and $\overline{E}$ calculated by equations (17) and (16). The magnitudes of the components of $\overline{E}$ (ΔH, $\Delta \alpha$, $\Delta \beta$, and $\Delta \gamma$) are then compared with a maximum change to be allowed. If any components exceed these maxima, A is adjusted and $\overline{E}$ recomputed. The maxima are reduced as the solution approaches the optimum. A 5-percent change in groove parameters was generally the maximum allowed at the beginning of the optimization procedure. At each iteration, Λ_m is recalculated by using a Newton-Raphson root finder.

RESULTS

Tables I and II present optimum herringbone groove parameters (H, α, β, and γ) to maximize stability over the range from $\Lambda = 0$ to the Λ value listed in the tables. Table I is for bearings with the smooth member rotating, and table II is for bearings with the grooved member rotating. The tables cover an operating range from incompressible lubrication ($\Lambda = 0$) to $\Lambda = 80$ and length-to-diameter ratios of 1/4, 1/2, 1, and 2. In addition to the resultant stability, the tables show the calculated radial load component F_r and the ratios of stability and load to the respective quantities of the maximum-load bearings of reference 5. Figures 4 to 9 are plotted from the data in tables I and II. The maximum groove depth ratio considered was $H = 4$, and the maximum groove width ratio was $\alpha = 0.6$. These were considered to be reasonable upper limits for practical bearing manufacture.

Tables I and II show that the improvement in stability over that of the maximum-load bearing generally increases with compressibility number and decreases with increasing length-to-diameter ratio. Stability improvement is greater for the bearing with the grooved member rotating. For $\Lambda = 80$ and $L/D = 1/4$ and 1/2, the stability increase is over three orders of magnitude.

For the case of $L/D = 1$ with the smooth member rotating, two local optima were observed at $\Lambda = 80$. The one shown in table I is that which gave the greater stability. It is possible that more than one local optimum exists for other cases as well. It was considered impractical to survey the entire possible range of all of the four parameters (H, α, β, and γ) to determine optimum values. Instead, the optimization procedure was started from the maximum-load solution (ref. 5) for the incompressible case. For $\Lambda = 1$ and higher, the optimization was started from the stability solution for the next

10

lower Λ. It is felt that the use of this method is justified by the results, since the groove parameters determined yield bearings substantially more stable than the maximum-load bearings of reference 5.

Radial load capacity, relative to the maximum-load bearings, decreases with increasing compressibility number. In contrast to the thousandfold increase in stability, however, the greatest loss in load capacity is 77 percent.

Figure 4 shows the stability attained by the optimized bearings. Stability with the grooved member rotating is always higher than with the smooth member rotating. The difference becomes greater at higher compressibility numbers. The greatest difference is at $\Lambda = 80$ for $L/D = 1$, where the stability of the bearing with the grooved member rotating is some 77 times that of the bearing with the smooth member rotating.

There are horizontal portions in each of the stability curves for the grooved member rotating. These occur because of the nonmonotonic behavior of the stability with compressibility number, as illustrated in figure 3(b). For compressibility numbers just to the right of the relative minimum in the curve, the governing stability over the range from 0 to the Λ of interest is the stability at the minimum, as discussed in the section OPTIMIZING PROCEDURE.

As shown by the solid curve of figure 3(b), stability changes very rapidly with compressibility number at high Λ. This means that, practically, there is a limiting compressibility number beyond which instability ensues for any value of M. To the authors' knowledge, instability in this region of the stability map has not been observed experimentally. Reference 11 does report several cases of sudden seizures of bearings operated near this stability boundary. However, the causes could have been factors other than instability, such as loss of clearance due to thermal growth of the journal.

It should also be noted that stability is quite sensitive to changes in groove parameters. The greatest sensitivity appears to be to groove length. For example, for the bearing optimized for $L/D = 1$ and $\Lambda = 80$ with the grooved member rotating, a 0.4-percent decrease in groove length produces a 27-percent increase in stability at $\Lambda = 80$. Because of this sensitivity and the manufacturing tolerances that must be allowed, a conservative design (M less than the theoretical stability limit by a factor of 2 or more) is recommended for bearings with the grooved member rotating at high Λ.

Radial load capacities of the optimized bearings are shown in figure 5. In common with the maximum-load bearings of reference 5, the optimized bearings show generally increasing radial load capacity with increasing length-to-diameter ratio and higher values when the smooth member rotates.

Figures 6 to 9 plot the optimum groove parameters as a function of compressibility number. It may be noted that, except for groove length ratio γ, the parameters for the bearing with the grooved member rotating generally vary over a much wider range than those for the bearing with the smooth member rotating. Again, this is believed to be the result of the nonmonotonic behavior of the stability curves, as discussed previously.

Groove length ratio is an exception to this wider variability. The fully grooved bearing ($\gamma = 1$) was optimum for nearly all the cases studied when the grooved member rotated. Experimental data (ref. 3) appear to verify this result.

CONCLUDING REMARKS

Optimum groove configurations were determined to maximize the stability of herringbone-grooved journal bearings. Design curves presented enable one to find the optimum herringbone bearing for a wide range of operating conditions. These range from incompressible lubrication to gas lubrication at high compressibility numbers for either the smooth or grooved member rotating and for length-to-diameter ratios of 1/4, 1/2, 1, and 2.

Bearings with the grooved member rotating are substantially more stable than those with the smooth member rotating, especially at high compressibility numbers. The bearing configurations derived in this report are also much more stable than bearings optimized for load capacity. Again, the stability increase is greater at higher compressibility numbers.

Lewis Research Center,
    National Aeronautics and Space Administration,
        Cleveland, Ohio, August 1, 1974,
            501-24.

APPENDIX - COEFFICIENTS FOR HERRINGBONE BEARING EQUATIONS

The following equations define the coefficients used in equations (3), (4), and (6):

$$C_p = \frac{\alpha(1-\alpha)(H^3-1)(H-1)\sin\beta\cos\beta}{H^3 + \alpha(1-\alpha)(H^3-1)^2\sin^2\beta}\,\Lambda\,\frac{L}{R}$$

$$C_1 = \frac{H^3 + \alpha(1-\alpha)(H^3-1)^2\sin^2\beta}{\alpha+(1-\alpha)H^3}\,\frac{R}{L}\,\frac{p_0}{p_a}$$

$$C_2 = \frac{\alpha(1-\alpha)(H^3-1)(H-1)\sin\beta\cos\beta}{\alpha+(1-\alpha)H^3}\,\Lambda$$

$$C_3 = \frac{2\xi\alpha(1-\alpha)(H^3-1)^2\sin\beta\cos\beta}{\alpha+(1-\alpha)H^3}\,\frac{p_0}{p_a}$$

$$C_4 = C_3 C_p\,\frac{p_a}{p_0} + \frac{\alpha(1-\alpha)(H^3-1)(H-1)\sin^2\beta}{\alpha+(1-\alpha)H^3}\,\xi\Lambda\,\frac{L}{R} - (1-\alpha+\alpha H)\Lambda\,\frac{L}{R}\left(1-\frac{2\omega_p}{\omega}\right)$$

$$C_5 = \frac{H^3 + \alpha(1-\alpha)(H^3-1)^2\cos^2\beta}{\alpha+(1-\alpha)H^3}\,\frac{L}{R}\,\frac{p_0}{p_a}$$

$$C_6 = \left(\frac{-3\xi\alpha(1-\alpha)(H-1)^2\sin^2\beta}{\left[\alpha+(1-\alpha)H^3\right]^2}\right.$$

$$\left.\times\left\{\frac{\alpha(1-\alpha)(H^3-1)^2\cos^2\beta[(1-\alpha)H^2(H^2+H-1)-\alpha(H^2-H-1)]}{H^3+\alpha(1-\alpha)(H^3-1)^2\sin^2\beta}-H^2\right\}+\left(1-\frac{2\omega_p}{\omega}\right)\right)\Lambda\,\frac{L}{R}$$

$$C_7 = \frac{3C_p^2(H^2-1)}{\left[\alpha+(1-\alpha)H^3\right](H^3-1)}\left[H^2(H^2+1)+\alpha(1-\alpha)(H^3-1)^2\sin^2\beta\right]\frac{R}{L}$$

REFERENCES

1. Vohr, J. H.; and Chow, C. Y.: Characteristics of Herringbone-Grooved, Gas-Lubricated Journal Bearings. J. Basic Eng., vol. 87, no. 3, Sept. 1965, pp. 568-578.

2. Malanoski, S. B.: Experiments on an Ultrastable Gas Journal Bearing. J. Lubri. Tech., vol. 89, no. 4, Oct. 1967, pp. 433-438.

3. Cunningham, Robert E.; Fleming, David P.; and Anderson, William J.: Experimental Stability Studies of the Herringbone-Grooved Gas-Lubricated Journal Bearing. J. Lubri. Tech., vol. 91, no. 1, Jan. 1969, pp. 52-59.

4. Cunningham, Robert E.; Fleming, David P.; and Anderson, William J.: Experimental Load Capacity and Power Loss of Herringbone-Grooved Gas-Lubricated Journal Bearings. J. Lubri. Tech., vol. 93, no. 3, July 1971, pp. 415-422.

5. Hamrock, Bernard J.; and Fleming, David P.: Optimization of Self-Acting Herringbone Journal Bearings for Maximum Radial Load Capacity. NASA TN D-6351, 1971.

6. Rieger, N. F., ed.: Design of Gas Bearings. Vol. 1: Design Notes. Mechanical Technology, Inc., 1966, p. 6.1.35.

7. Fleming, David P.: Steady-State and Stability Analysis of Externally Pressurized Gas-Lubricated Journal Bearings With Herringbone Grooves. NASA TN D-5870, 1970.

8. Pan, C. H. T.: Spectral Analysis of Gas Bearing Systems for Stability Studies. Dynamics and Fluid Mechanics. Vol. 3, Part 2 of Developments in Mechanics, T. C. Huang and M. W. Johnson, Jr., eds., John Wiley & Sons, Inc., 1965, pp. 431-447.

9. Scarborough, James B.: Numerical Mathematical Analysis. Sixth ed., Johns Hopkins Press, 1966.

10. Hamrock, Bernard J.: Optimization of Self-Acting Thrust Bearings for Load Capacity and Stiffness. NASA TN D-5954, 1970.

11. Kaneko, R.; Mitsuya, Y.; and Oguchi, S.: High-Speed Magnetic Storage Drums With Grooved Hydrodynamic Gas Bearings. Presented at 6th International Gas Bearing Symposium, BHRA Fluid Engineering, University of Southampton, Southampton, England, 1974.

TABLE I. - HERRINGBONE GROOVE PARAMETERS TO MAXIMIZE STABILITY

WITH SMOOTH MEMBER ROTATING

Solution	Film thickness ratio, H	Groove width ratio, α	Groove length ratio, γ	Groove angle, β, deg	Stability, M	Radial load capacity, F_r	Stability ratio[a]	Load ratio[b]
Length-to-diameter ratio L/D, 1/4								
Incompressible	2.68	0.469	0.764	18.6	5.16	0.0366	1.07	0.96
Compressible, for Λ[c] of -								
1	2.67	0.466	0.755	18.5	5.11	0.0366	1.09	0.96
5	2.62	.454	.720	18.4	.977	.182	1.15	.94
10	2.57	.441	.678	18.3	.464	.359	1.30	.92
20	2.52	.421	.604	18.2	.210	.686	2.44	.88
40	2.47	.397	.481	17.8	.0884	1.20	155	.80
80	2.5	.38	.32	18	.0329	1.77	571	.66
Length-to-diameter ratio L/D, 1/2								
Incompressible	2.54	0.475	0.736	21.3	9.32	0.653	' 1.04	0.98
Compressible, for Λ[c] of -								
1	2.53	0.471	0.721	21.1	9.14	0.0667	1.05	0.97
5	2.47	.453	.663	20.6	1.70	.354	1.08	.96
10	2.44	.436	.600	20.1	.783	.718	1.15	.95
20	2.42	.411	.493	19.1	.336	1.29	4.27	.93
40	2.48	.392	.339	18.2	.129	1.85	72	.80
80	2.12	.34	.26	15	.0406	2.08	100	.55
Length-to-diameter ratio L/D, 1								
Incompressible	2.37	0.493	0.685	26.0	14.3	0.0992	1.02	0.98
Compressible, for Λ[c] of -								
1	2.36	0.488	0.663	25.7	13.9	0.116	1.10	0.96
5	2.31	.471	.591	24.5	2.50	.735	3.13	.84
10	2.30	.454	.516	23.2	1.12	1.33	1.06	.98
20	2.32	.425	.410	20.7	.463	1.91	2.86	.93
40	2.52	.398	.263	19.4	.170	2.47	6.91	.76
80	3.77	.158	.268	9.7	.0510	2.81	3.83	.50
Length-to-diameter ratio L/D, 2								
Incompressible	2.25	0.528	0.636	32.6	16.1	0.112	1.02	0.99
Compressible, for Λ[c] of -								
1	2.24	0.528	0.607	32.1	15.4	0.203	∞	0.57
5	2.19	.527	.527	30.4	2.68	1.21	1.32	.91
10	2.18	.526	.467	28.9	1.19	1.86	1.05	.98
20	2.22	.528	.398	25.9	.509	2.67	1.22	.90
40	2.23	.500	.346	24.8	.212	3.93	1.43	.79
80	2.29	.461	.332	23.4	.0881	6.43	1.65	.71

[a]Stability of maximum-stability bearing/stability of maximum-load bearing.

[b]Radial load capacity of maximum-stability bearing/radial load capacity of maximum-load bearing.

[c]Bearing compressibility number.

TABLE II. - HERRINGBONE GROOVE PARAMETERS TO MAXIMIZE STABILITY

WITH GROOVED MEMBER ROTATING

[Maximum H considered, 4; maximum α considered, 0.6.]

Solution	Film thickness ratio, H	Groove width ratio, α	Groove length ratio, γ	Groove angle, β, deg	Stability, M	Radial load capacity, F_r	Stability ratio[a]	Load ratio[b]
Length-to-diameter ratio L/D, 1/4								
Incompressible	4	0.6	1	11.4	8.64	0.0314	1.38	0.83
Compressible, for Λ^c of -								
1	4	0.6	1	11.7	9.79	0.0313	1.52	0.82
2	4			11.9	5.71	.0626	1.73	.82
5	4			12.2	4.41	.155	3.43	.80
10	4			12.2	4.41	.305	5.12	.79
20	2.40			32.4	1.37	.647	2.03	.85
40	1.99			59.0	.450	.750	417	.54
80	1.94			74.4	.125	.733	1640	.31
Length-to-diameter ratio L/D, 1/2								
Incompressible	2.59	0.6	1	23.4	11.9	0.0629	1.14	0.94
Compressible, for Λ^c of -								
1	2.99	0.6	1	19.6	13.1	0.0592	1.24	0.86
2	4	.6		13.7	8.02	.0865	1.50	.61
5		.6		14.0	7.28	.210	6.26	.57
10		.567		11.8	5.74	.368	5.58	.50
20		.361		11.8	2.30	.638	3.66	.49
40		.295		10.0	1.14	.960	467	.48
80		.317		8.69	.951	1.32	3880	.45
Length-to-diameter ratio L/D, 1								
Incompressible	2.17	0.6	1	36.0	16.6	0.0899	1.10	0.89
Compressible, for Λ^c of -								
1	2.25	0.6	1	36.2	18.4	0.0973	1.39	0.79
2	2.37			35.6	10.6	.194	∞	.61
5	2.54			34.1	8.61	.424	13.6	.49
10	2.54			34.1	8.61	.654	8.52	.49
20	3.10			22.0	6.44	.694	9.47	.37
40	3.06			21.8	6.39	.997	299	.37
80	2.77	.478	.904	24.2	3.94	2.87	779	.68
Length-to-diameter ratio L/D, 2								
Incompressible	2.06	0.6	0.831	43.1	17.7	0.107	1.04	0.94
Compressible, for Λ^c of -								
1	2.12	0.6	0.900	46.6	18.6	0.150	∞	0.42
2	2.22		.976	50.3	10.0	.278	∞	.37
5	2.46		1	54.4	6.19	.461	3.31	.35
10	2.50		1	55.0	6.14	.626	5.29	.35
20	2.54		1	57.6	5.99	.830	10.1	.32
40	2.68		1	63.7	4.71	1.00	19.4	.24
80	2.68		.949	66.1	3.72	1.69	42.7	.23

[a] Stability of maximum-stability bearing/stability of maximum-load bearing.

[b] Radial load capacity of maximum-stability bearing/radial load capacity of maximum-load bearing.

[c] Bearing compressibility number.

16
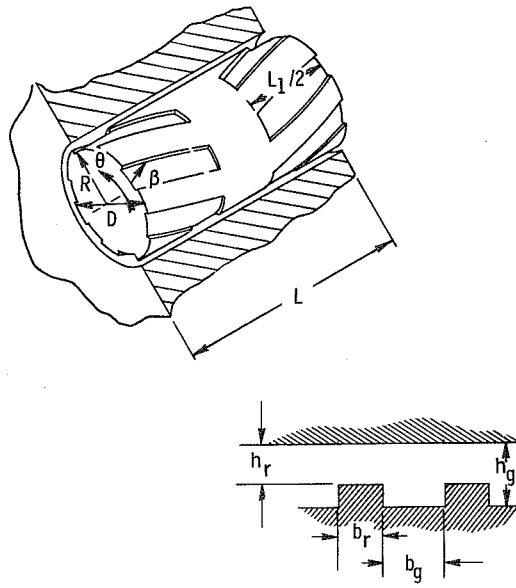
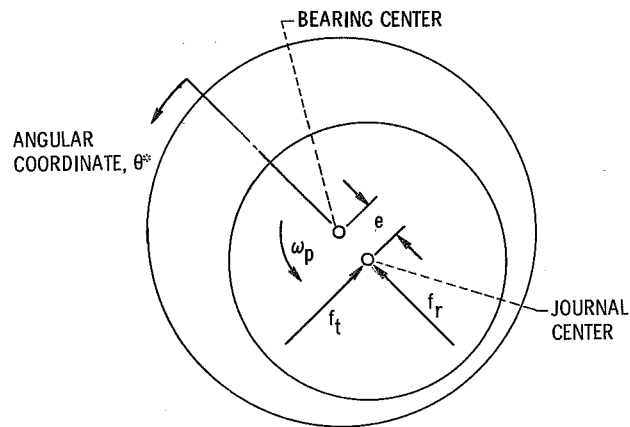Figure 1. – Schematic of concentric herringbone journal
bearing.

Figure 2. – Whirling journal bearing.

(a) SMOOTH MEMBER ROTATING.
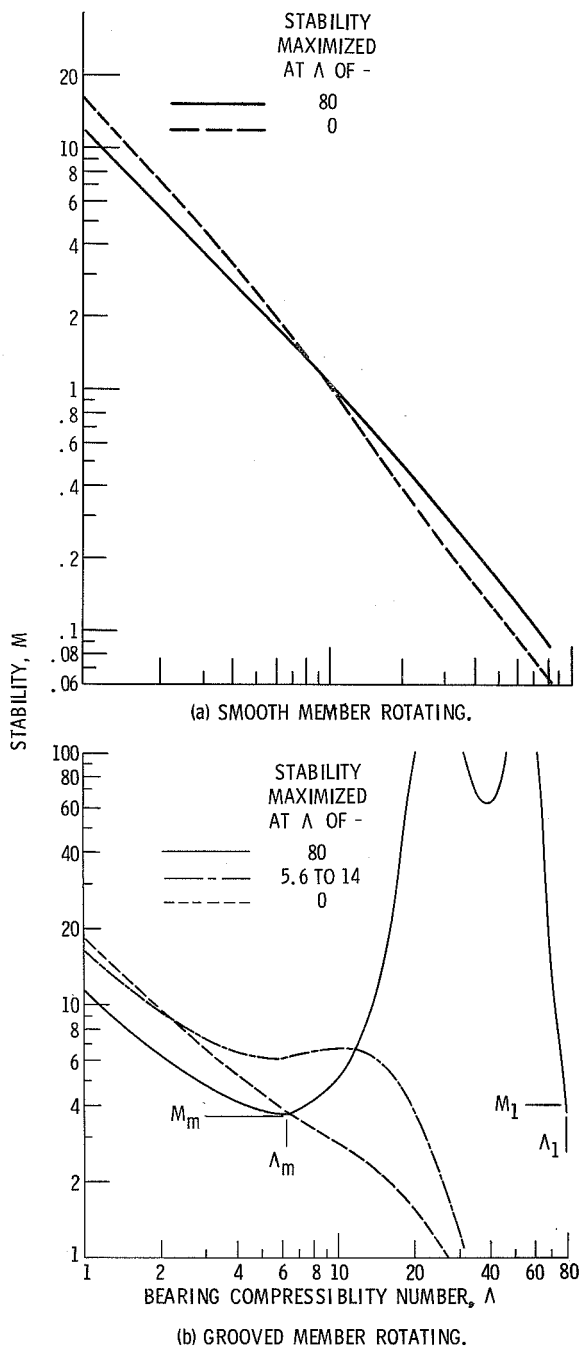
(b) GROOVED MEMBER ROTATING.

Figure 3. - Typical stability curves for optimized bearings. Length-to-diameter ratio, 2.
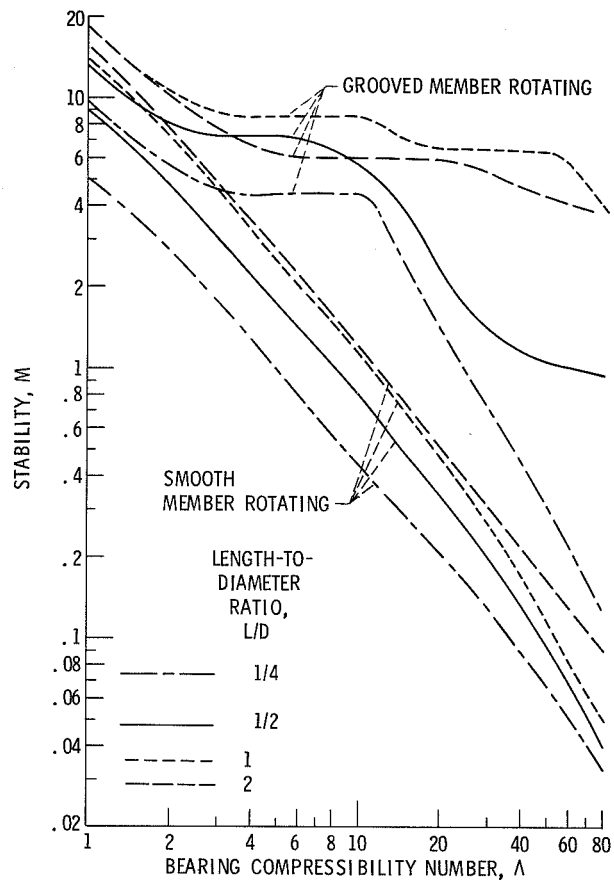
Figure 4. - Maximum stability of herringbone-grooved bearings.
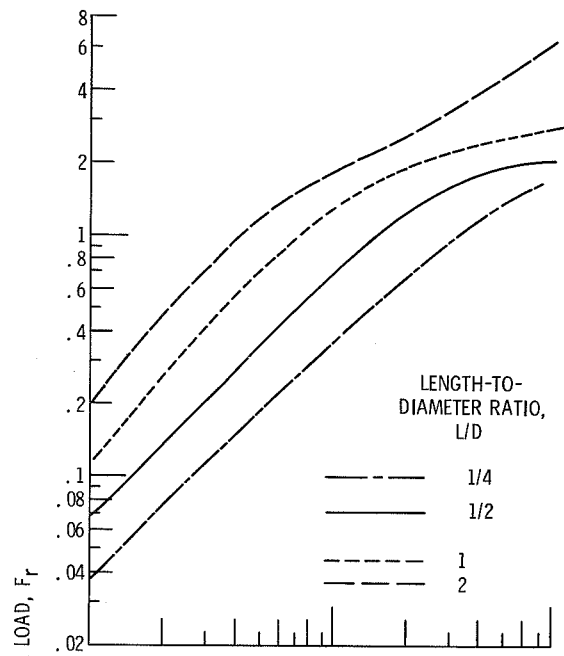
Figure 5. - Radial load capacity of maximum-stability bearings.

(a) SMOOTH MEMBER ROTATING.
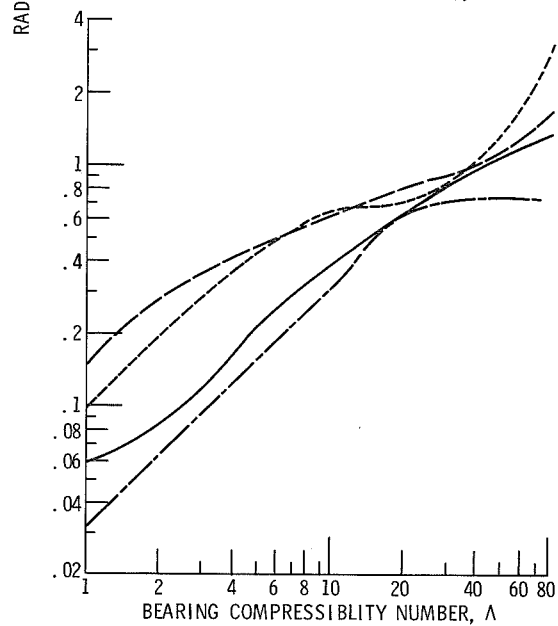
(b) GROOVED MEMBER ROTATING.
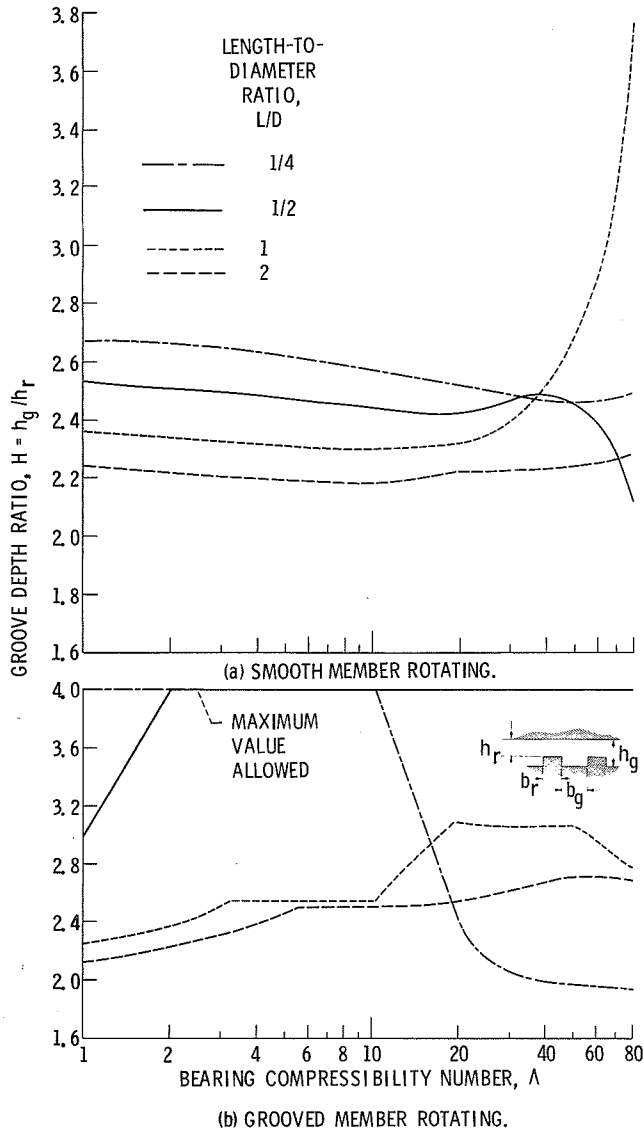
Figure 6. - Groove depth ratios to maximize stability.
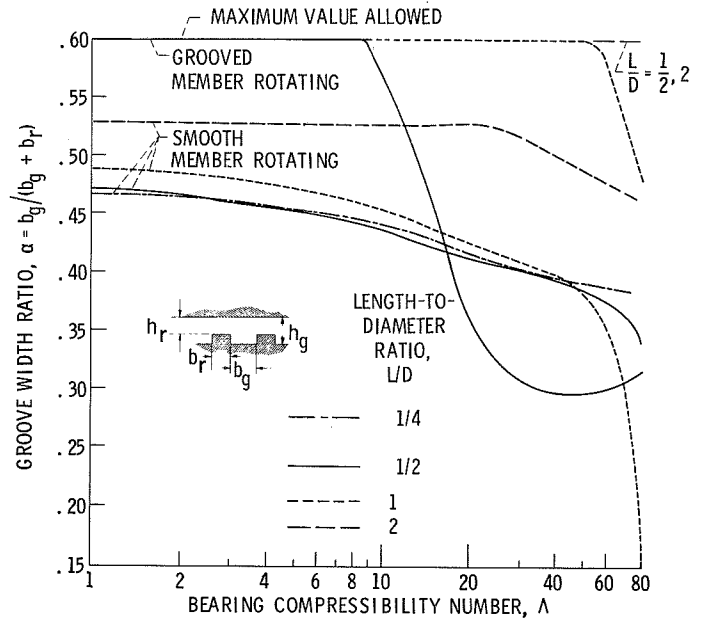
Figure 7. - Groove width ratios to maximize stability.

(a) SMOOTH MEMBER ROTATING.
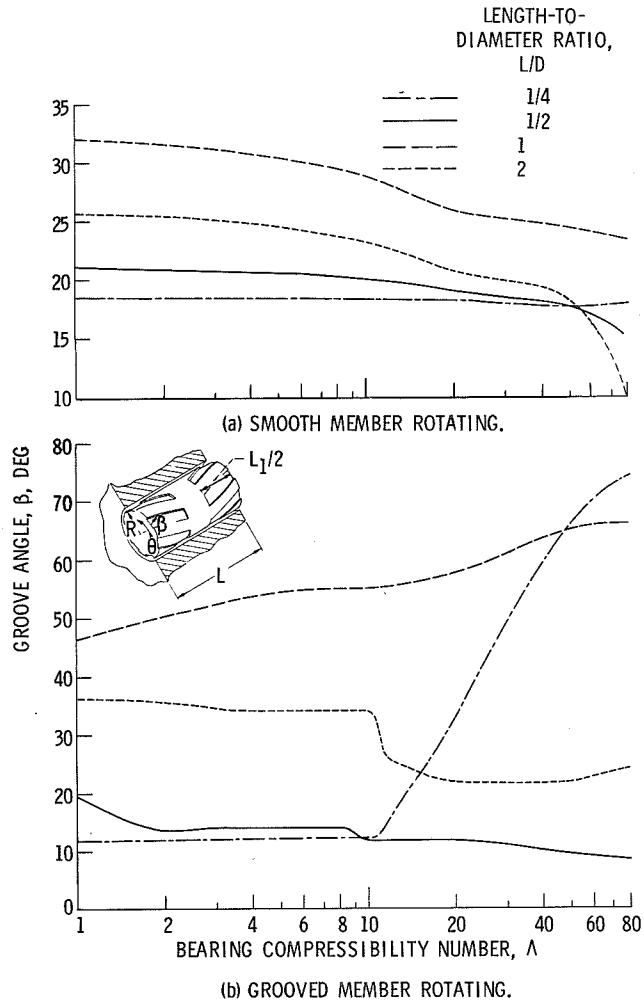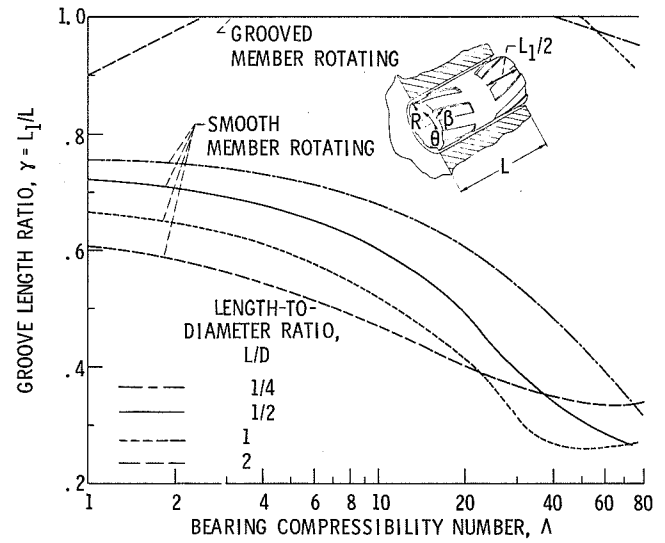
(b) GROOVED MEMBER ROTATING.

Figure 8. – Groove angles to maximize stability.

Figure 9. – Groove length ratios to maximize stability.